Single-ion anisotropy, Dzyaloshinskii-Moriya interaction, and negative magnetoresistance of the spin-1/2 pyrochlore $R_{2}V_{2}O_{7}$

H. J. Xiang, E. J. Kan, M.-H. Whangbo, C. Lee, Su-Huai Wei, and X. G. Gong

Single-ion anisotropy, Dzyaloshinskii-Moriya interaction and negative magnetoresistance of the spin-1/2 pyrochlores $R_2V_2O_7$

H. J. Xiang,[1] E. J. Kan,[2] M.-H. Whangbo,[2] C. Lee,[2] Su-Huai Wei,[3] and X. G. Gong[1]

[1]*Key Laboratory of Computational Physical Sciences (Ministry of Education),*

and Department of Physics, Fudan University, Shanghai 200433, P. R. China

[2]*Department of Chemistry, North Carolina State University,*

Raleigh, North Carolina 27695-8204, USA

[3]*National Renewable Energy Laboratory, Golden, Colorado 80401, USA*

Abstract

The electronic and magnetic properties of spin-1/2 pyrochlores $R_2V_2O_7$ were investigated on the basis of density-functional calculations. Contrary to the common belief, the spin-1/2 V^{4+} ions are found to have a substantial easy-axis single-ion anisotropy. We show that the magnon quantum Hall effect of $Lu_2V_2O_7$ is a combined consequence of the easy-axis single-ion anisotropy and the Dzyaloshinskii-Moriya interaction of the spin-1/2 V^{4+} ions. We also show that the negative magnetoresistance observed for $R_2V_2O_7$ arises from a new mechanism, i.e., the band gap decreases as the spin alignment becomes more parallel to each other.

PACS numbers: 75.30.Gw,71.15.Rf,71.20.-b,75.10.-b

I. INTRODUCTION

During the past two decades the magnetic properties of pyrochlore oxides of the type $R_2^{3+}M_2^{4+}O_7$ (R = rare-earth; M = transition metal) have been extensively studied[1,2], due largely to the spin frustration in the pyrochlore lattice that results when the nearest-neighbor (NN) spin exchange is antiferromagnetic (AFM)[1]. The vanadate pyrochlores $R_2V_2O_7$ (R = Lu, Yb, Tm, Y) are unique because they are ferromagnetic insulators[3–8] contrary to the observation that ferromagnetism leads usually to metallic character. Furthermore, $Lu_2V_2O_7$ exhibits a negative magnetoresistance (MR) as high as 50% just above the Curie temperature $T_C = 73K$ under magnetic field of 5 T[9]. Recently, $Lu_2V_2O_7$ is found to exhibit a magnon Hall effect (i.e., the anomalous thermal Hall effect caused by spin excitations)[10]. The explanations presented for these observations raise fundamental questions. Namely, the MR of $Lu_2V_2O_7$ was suggested to be caused by polaron mediation as found in $Tl_2Mn_2O_7$[9]. However, this possibility seems remote, because the diffuse $6s$ orbital of the Tl^{3+} ion is believed to assist the polaron formation in $Tl_2Mn_2O_7$ whereas the Lu^{3+} ion in $Lu_2V_2O_7$ does not have such an extended s orbital. In the magnon Hall effect[11], the Dzyaloshinskii-Moriya (DM) interaction is considered to play the role of the vector potential as in the intrinsic anomalous Hall effect in metallic ferromagnets. In the fitting analysis of their experimental data, Onose *et al.* found it necessary to use the $|D/J|$ ratio of 0.32. This ratio is unusually large because the DM interaction is a consequence of spin-orbit coupling (SOC) so that the typical $|D/J|$ ratio is expected to be smaller than 0.1. Therefore, it is important to quantify the magnitude of the DM term. In this work, we probe these questions by studying the electronic and magnetic properties of $R_2V_2O_7$ on the basis of density functional calculations to find that the spin-1/2 V^{4+} ions have a substantial easy-axis single-ion anisotropy contrary to the common belief, the neglect of this anisotropy can lead to an unusually large $|D/J|$ ratio, and $R_2V_2O_7$ exhibits a new type of negative MR mechanism.

II. COMPUTATIONAL METHODS

Our calculations are based on the density functional theory (DFT) plus the on-site re-pulsion (U) method[12] (DFT+U) within the generalized gradient approximation[13] on the basis of the projector augmented wave method[14] encoded in the Vienna ab initio simula-

tion package[15]. The plane-wave cutoff energy was set to 400 eV. Careful convergence test were performed and the total energy was converged to 10^{-6} eV. In the following, we report results obtained with U = 3 eV and J = 1 eV on V, but the dependence of our results on U and J will be also discussed. It was found[16] that $Y_2V_2O_7$ has magnetic properties very similar to those of $Lu_2V_2O_7$. Unlike the case of $Y_2V_2O_7$, our calculations for $Lu_2V_2O_7$ led to some convergence difficulties so that our calculations focused mainly on $Y_2V_2O_7$ using its experimental structure[16]. The structural optimization was found to have a negligible effect on its magnetic properties.

III.   RESULTS AND DISCUSSION

In the V_2O_7 framework of $Y_2V_2O_7$ (space group $Fd\bar{3}m$), the VO_6 octahedron containing V^{4+} ($3d^1$, $S = 1/2$) ions share their corners such that the V^{4+} ions form corner-sharing V_4 tetrahedrons [see Fig. 1(a)]. The localized $S = 1/2$ spins at the V^{4+} sites order ferromagnetically below $T_C \sim 70$ K. The VO_6 octahedron of $R_2V_2O_7$ are slightly distorted (i.e., axially-compressed slightly) from the ideal shape. Under the trigonal crystal field, the t_{2g} states are split into the lowest a_{1g} state $|0\rangle$ and two e'_g states $|+\rangle$ and $|-\rangle$[7]:

$$
\begin{aligned}
|0\rangle &= 1/\sqrt{3}(d_{xy} + d_{yz} + d_{xz}) \\
|+\rangle &= -1/\sqrt{3}(d_{xy} + e^{2\pi i/3}d_{yz} + e^{-2\pi i/3}d_x) \\
|-\rangle &= 1/\sqrt{3}(d_{xy} + e^{-2\pi i/3}d_{yz} + e^{2\pi i/3}d_{xz}),
\end{aligned}
\tag{1}
$$

where the (x, y, z) coordinate system refers to the local coordinate adopted for a perfect VO_6 octahedron [see Fig. 1(c)]. Note that the higher e_g states $d_{x^2-y^2}$ and d_{z^2} remain degenerate. The recent polarized neutron diffraction study[5] showed that, at each V site of a given V_4 tetrahedron, only the a_{1g} level is occupied by an electron.

The band structure and density of states calculated for the ferromagnetic (FM) state of $Y_2V_2O_7$ by the DFT+U method are shown in Fig. 2(a) and Fig. 3(a), respectively. Both the valence band maximum (VBM) and conduction band minimum (CBM) are majority-spin states. There is an indirect band gap of about 0.33 eV between the VBM state near the W point and the CBM state at the Γ point. This band gap is consistent with the experimentally measured activation energy 0.2 eV[3]. Our calculations show that the FM state of $Y_2V_2O_7$ has a nonzero band gap when $U - J \geq 1.5$ eV. The four states between -0.7 eV and 0 eV (with zero set at the VBM level) are the occupied $3d$ states of the four V^{4+} ions per unit cell.

3

The electron density associated with the four states, plotted in the inset of Fig. 3(a), clearly shows that these occupied orbitals are the a_{1g} states, in agreement with experiment[5,6]. The analysis of the partial density of states provides further insight into the electronic structures of $Y_2V_2O_7$. For the spin majority part, the orbital levels are consistent with the trigonal crystal field splitting. For the spin minority part, the empty $|+\rangle$ and $|-\rangle$ states have lower energies than the unoccupied $|0\rangle$ state. This is so because the intra-orbital onsite Coulomb interaction U is much larger than the interorbital onsite Coulomb interaction (U'), and the trigonal crystal field splitting between the a_{1g} and e'_g states. The spin down a_{1g} state lies slightly lower in energy than the spin down e_g states, and both states are delocalized with strong hybridization between them. The electron configuration of the V^{4+} ion is shown schematically in Fig. 3(b).

The symmetric spin exchange parameters were extracted by mapping the energy differences between ordered collinear spin states obtained from DFT+U calculations onto the corresponding energy differences obtained from the quantum Heisenberg Hamiltonian for the spin-1/2 system: $H = \sum_{i<j} J_{ij}\hat{\mathbf{S}}_i \cdot \hat{\mathbf{S}}_j$. We consider all symmetric spin exchange interactions up to the third nearest neighboring pairs [see Fig. 1(b)]; the NN exchange J_1 within each V_4 tetrahedron and the next NN exchanges J_2, J_3 and J_4. To evaluate these four spin exchange parameters reliably, we considered 33 different ordered spin states and then determined them by performing a linear least-square fitting analysis[17]. Our calculations show that $J_1 = -7.09$ meV, $J_2 = -0.07$ meV, $J_3 = -0.31$ meV, and $J_4 = -0.28$ meV, namely, J_2, J_3 and J_4 are negligibly small compared with the NN FM exchange J_1. Using the calculated J_1, we estimate the Curie-Weiss temperature $\theta = zS(S+1)J_1/3k_B = 6 \times \frac{1}{2}(\frac{1}{2}+1)J_1/3k_B = 122$ K, which is close to the observed value 106 K for $Lu_2V_2O_7$[9]. The calculated spin exchange parameters show that the magnetic ground state is the FM state, in agreement with experiment. Interestingly, we find that J_1 is always ferromagnetic for any reasonable U and J values ($U < 8$ and $J \geq 0$), which is not in support of the previous prediction[5] that antiferromagnetism is favorable when $J < 0.7$.

The ferromagnetism in $R_2V_2O_7$ can be understood by comparing the electron hopping processes between adjacent spin sites 1 and 2 for cases when they have the FM and AFM arrangements. In the FM case, the electron in the $a_{1g}^{1\uparrow}$ state can hop to the majority-spin e'_g and e_g states, but not to a_{1g} state, of site 2. In the AFM case, the electron in the $a_{1g}^{1\uparrow}$ can hop to all minority-spin states of site 2. The energy gain from the virtual hopping is larger

for the FM than for the AFM case, because the empty degenerate up-spin states of site 2 are closer in energy to the filled $a_{1g}^{1\uparrow}$ state for the FM case. The hopping between $a_{1g}^{1\uparrow}$ state and the minority-spin a_{1g} state of site 2 in the AFM arrangement is negligible because the two states have a large energy gap and a rather small transfer integral.

Fig. 2(b) shows the band structure of an AFM state in which there are two up- and two down-spins in every V_4 tetrahedron [see inset of Fig. 2(b)]. As in the FM case, there is an indirect band gap between the VBM state near the W point and the CBM state at the Γ point. However, there is an important difference: The band gap of the AFM state is about 0.62 eV, which is almost twice that of the FM state. By taking the level of the Y $4s$ semicore level as the reference, we find that the VBM level of the FM state is at almost the same (only about 0.01 eV higher) as that of the AFM state. Therefore, the CBM of the AFM state is much higher than that of the FM state. The reason why the AFM state has a higher CBM and thus a larger band gap is illustrated in Fig. 3(d). When the spins of two neighboring V ions have an FM coupling, the up-spin e_g' states of the adjacent sites have the same energies so that the lowest energy state is lower than the e_g' level by t', where t' is the hopping integral between the adjacent e_g' states. In the AFM case, however, the lowest energy state is lower than the majority-spin e_g' level by t'^2/Δ, where Δ is the exchange splitting and $\Delta > t'$. Therefore, the AFM state has a higher CBM and thus a larger band gap. This fact naturally explains the negative MR observed just above the ferromagnetic Curie temperature T_c. When the temperature is lowered towards T_C, the spins have a tendency to order ferromagnetically, but are not fully aligned. The application of an external magnetic field (about 5 T) will help align the spins ferromagnetically. Thus, the band gap decreases with increasing the magnetization, so that the resistivity of $R_2V_2O_7$ would be reduced by external magnetic field hence leading to the negative MR effect. This explanation is consistent with the observation that the maximum MR effect occurs at 75 K, right above the Curie temperature [See Fig. 3(a) of Ref.[9]]. We note that this new mechanism of negative MR should be also applicable to other ferromagnetic insulators (e.g., EuO).

Let us now examine the magnetic properties that require the consideration of SOC. For two interacting spins, the SOC can induce DM antisymmetric interactions $H_{DM} = \mathbf{D}_{ij} \cdot (\hat{\mathbf{S}}_i \times \hat{\mathbf{S}}_j)$ ($\mathbf{D}_{ij} = D\mathbf{d}_{ij}$, $D = |\mathbf{D}_{ij}|$ and $\mathbf{d}_{ij}$ is a unit vector). According to the crystal symmetry, the DM vector for a V-V edge of each V_4 tetrahedron is perpendicular to the V-V bond and is parallel to the opposite edge of the V_4 tetrahedron [Fig. 1(d)]. To evaluate

the magnitude of the DM interaction term D, we consider two spin configurations shown in Fig. 1(e). In one spin configuration, the four spins are aligned along the X, Y, Z, and Z axes, respectively [see Fig. 1(a) for the definition of the global coordinate system XYZ]. From this configuration, we generate the other spin configuration by performing a reflection operation of each spin with respect to the XZ plane containing the spin site. The only difference from the first configuration is that the spin at the second site now points along the $-Y$ direction. It can be easily shown that the two spin configurations have the same spin exchange interactions and the same single-ion anisotropy interactions (see below). In terms of the quantum expression of the DM interaction Hamiltonian, it is found that the total DM interaction vanishes for the first spin configuration, but is $D\sqrt{2}/2$ per V_4 tetrahedron for the second spin configuration. By using the energy difference between the two spin configurations obtained from the DFT+U+SOC calculations, D is estimated to be 0.34 meV. The D value is rather insensitive to the calculation parameters (U and J). Consequently, D is of the order of 5% of the NN spin exchange $J_1 = -7.09$ meV, i.e., $|D/J_1| = 0.048$, which is almost an order of magnitude smaller than the value $D/J_1 = 0.32$ deduced by Onose *et al.* from analyzing the magnetic field dependence of the thermal Hall conductivity in terms of their model for the magnon Hall effect. To test the reliability of our estimation for D, we calculated the energies of two spin configurations, i.e., one with four spins along the X, X, Z, and Z axes, and the other with four spins along the X, X, $-Z$, and $-Z$ axes. These two spin configurations have the same DM interaction energy due to the same symmetric exchange energy and the same single-site anisotropy energy. The energy difference between the two configurations is calculated to be 0.003 meV. The latter is negligible compared with the energy difference between spin configurations used to extract the DM parameters. Thus, the D/J_1 ratio we calculate is reliable. This raises a serious question as to whether the observed thermal Hall effect can be described solely in terms of the DM interaction.

Another important consequence of the SOC interaction is that the magnetic moment of each spin site gets a preferred orientation in space with respect to the crystal lattice. However, it is commonly believed that a spin-1/2 ion has no single-ion anisotropy because the spin doublet state is not split by the zero-field splitting term $CS_z^2 = CI/4$ for $S = 1/2$ (C is a constant and I is a 2×2 unit matrix)[18]. Here, we find that the spin-1/2 V ions of $R_2V_2O_7$ have substantial single-ion anisotropy, which is not described by the usual zero-field splitting

6

term. The single-ion anisotropy of the V^{4+} ion can be estimated in two ways. First, we replace three of the four V^{4+} ions in each V_4 tetrahedron of $Y_2V_2O_7$ with non-magnetic Ti^{4+} Ti^{4+} ions to obtain $Y_2Ti_{\frac{3}{2}}V_{\frac{1}{2}}O_7$, which has no NN pairs of V^{4+} ions. Our DFT+U+SOC calculations show that the easy axis of the spin-1/2 V ion is along the three-fold rotational axis [z' in Fig. 1(c)] of the distorted VO_6 octahedron. The state with spin moments parallel to the z' axis is more stable than that with the spin moments perpendicular to the z'-axis by about 0.81 meV per V. Second, we consider two spin configurations to obtain a more accurate value of the single-ion anisotropy. In one configuration, all spins are along the easy axis directions such that, in a V_4 tetrahedron, one spin is pointed out from the center and the remaining three spins are pointed to the center. From this spin configuration, we obtain the other spin configuration by rotating the directions of all the spins around the global Z axis by 120°. In the resulting spin configuration all spins are perpendicular to the easy axis directions. The two spin configurations are the same in the symmetric exchange interactions and in the DM interactions. Our DFT+U+SOC calculations for the two spin configurations show that the spin orientation along the easy axis is more stable than that along the hard axis by 0.91 meV per V. Therefore, it is unequivocal that a spin-1/2 ion can have significant single-ion anisotropy, contrary to the general belief. It should be noted that single-ion anisotropy for a spin-1/2 ion is not excluded according to the general expression of the $\mathbf{L} \cdot \mathbf{S}$ Hamiltonian[18,20]. In the traditional effective spin Hamiltonian approach[18,19], the energy for an orbital/spin basis function $|LM_L\rangle|SM_S\rangle$ does not depend on the spin projection $|M_S\rangle$, whereas an exchange splitting is always present in any realistic magnetic system, as found in our first principles calculations. Unlike the case of $R_2V_2O_7$, the spin-1/2 Os^{7+} ion of Ba_2NaOsO_6 exhibits no single-ion anisotropy[21]. The two systems are different because the OsO_6 octahedron has an ideal shape and hence a triply-degenerate t_{2g} level whereas the VO_6 octahedron is slightly distorted from the ideal shape so that its t_{2g} level is split. We also calculated the single ion anisotropy of the spin-1/2 Cu^{2+} ion in the superconducting parent compound La_2CuO_4. In La_2CuO_4, the Cu ion is at the center of the distorted oxygen octahedron with two elongated Cu-O bonds. Our calculations show that the Cu^{2+} ion has an easy-plane anisotropy of 0.19 meV/Cu, which is smaller than the anisotropy (0.91 meV/V) found for the V^{4+} ion in $R_2V_2O_7$.

As described above, the single-ion anisotropy energy is much greater than the DM interaction parameter in $R_2V_2O_7$. We now estimate how the DM interaction parameter is affected

when the single-ion anisotropy energy is neglected. The single-ion anisotropy for the spin-$1/2$ V^{4+} ion cannot be described by any quantum spin Hamiltonian. Our calculations show that the single-ion anisotropy energy can nevertheless be written as $H_{ani} = A\sum_i(\mathbf{S}_i \cdot \mathbf{z}'_i)^2$ ($|\mathbf{S}| = 1/2$ and $A = -3.64$ meV) when the spins are treated as classical vectors. Then, the total classical spin Hamiltonian for $R_2V_2O_7$ is expressed as:

$$H = \sum_{i<j} J\mathbf{S}_i \cdot \mathbf{S}_j + D\sum_{i<j} \mathbf{d}_{ij} \cdot (\mathbf{S}_i \times \mathbf{S}_j) + A\sum_i(\mathbf{S}_i \cdot \mathbf{z}'_i)^2. \tag{2}$$

Using this classical spin Hamiltonian, our Monte Carlo simulation[22] shows that the spin ground state is nearly FM with the moments aligned along the [001] direction (shown in Fig. 4), which is in agreement with the slight anisotropy displayed in the magnetization curve[10]. If we renormalize the single ion anisotropy term into the DM interaction term, the Hamiltonian is rewritten as: $H = \sum_{i<j} J\mathbf{S}_i \cdot \mathbf{S}_j + D^{eff}\sum_{i<j} \mathbf{d}_{ij} \cdot (\mathbf{S}_i \times \mathbf{S}_j)$, where D^{eff} is the effective DM interaction parameter to be obtained by neglecting the single-ion anisotropy. For two spin configurations that are related to each other by a mirror-plane symmetry [e.g., see Fig. 1(e)], the energy differene can be used to extract D^{eff}. We generate several random spin configurations to find that $\frac{D^{eff}}{D}$ can be as large as 20. This shows that the effective DM interaction can be much larger than the actual DM interaction when the single-ion anisotropy is neglected.

IV. SUMMARY

In summary, $R_2V_2O_7$ exhibits negative MR because its band gap depends on the spin arrangement, with the smallest gap for the FM state. The V^{4+} ions of $R_2V_2O_7$ exhibits an easy-axis single-ion anisotropy that is much stronger than the DM interaction term D, despite the common belief that spin-$1/2$ have no single-ion anisotropy. The effective D value evaluated can be unreasonably large when this anisotropy is neglected, as found from the analysis of the magnon quantum Hall effect of $Lu_2V_2O_7$. Thus, the consideration of the single-ion anisotropy is necessary to formulate a more complete theory for the observed magnon Hall effect.

---

[1] J. S. Gardner, M. J. P. Gingras, and J. E. Greedan, Rev. Mod. Phys. **82**, 53 (2010).

[2] P. Blaha, D. J. Singh, and K. Schwarz, Phys. Rev. Lett. **93**, 216403 (2004).

[3] S. Shamoto, H. Tazawa, Y. Ono, T. Nakano, Y. Nozue, and T. Kajitani, J. Phys. Chem. Solids **62**, 325 (2001).

[4] S. Shamoto, T. Nakano, Y. Nozue, and T. Kajitani, J. Phys. Chem. Solids **63**, 1047 (2002).

[5] H. Ichikawa, L. Kano, M. Saitoh, S. Miyahara, N. Furukawa, J. Akimitsu, T. Yokoo, T. Matsumura, M. Takeda, and K. Hirota, J. Phys. Soc. Jpn. **74**, 1020 (2005).

[6] T. Kiyama, T. Shiraoka, M. Itoh, L. Kano, H. Ichikawa, and J. Akimitsu, Phys. Rev. B **73**, 184422 (2006).

[7] S. Miyahara, A. Murakami, and N. Furukawa, J. Mol. Struct. **838**, 223 (2007).

[8] G. T. Knoke, A. Niazi, J. M. Hill, and D. C. Johnston, Phys. Rev. B **76**, 054439 (2007).

[9] H. D. Zhou, E. S. Choi, J. A. Souza, J. Lu, Y. Xin, L. L. Lumata, B. S. Conner, L. Balicas, J. S. Brooks, J. J. Neumeier, and C. R. Wiebe, Phys. Rev. B **77**, 020411(R) (2008).

[10] Y. Onose, T. Ideue, H. Katsura, Y. Shiomi, N. Nagaosa, Y. Tokura, Science **329**, 297 (2010).

[11] H. Katsura, N. Nagaosa, and P. A. Lee, Phys. Rev. Lett. **104**, 066403 (2010).

[12] A. I. Liechtenstein, V. I. Anisimov, and J. Zaanen, Phys. Rev. B **52**, R5467 (1995).

[13] J. P. Perdew, K. Burke, and M. Ernzerhof, Phys. Rev. Lett. **77**, 3865 (1996).

[14] P. E. Blöchl, Phys. Rev. B **50**, 17953 (1994); G. Kresse and D. Joubert, *ibid* **59**, 1758 (1999).

[15] G. Kresse and J. Furthmüller, Comput. Mater. Sci. **6**, 15 (1996); Phys. Rev. B **54**, 11169 (1996).

[16] A. A. Haghighira, C. Gross, and W. Assmusd, J. Cryst. Growth **310**, 2277, 2008.

[17] H. J. Xiang, E. J. Kan, S.-H. Wei, M.-H. Whangbo, and J. L. Yang, Phys. Rev. B **80**, 132408 (2009).

[18] D. Dai, H. J. Xiang, and M.-H. Whangbo, J. Comput. Chem. **29**, 2187 (2008).

[19] Norberto Majlis, The Quantum Theory of Magnetism (World Scientific, Singapore, 2000).

[20] H. J. Xiang, S.-H. Wei, and M.-H. Whangbo, Phys. Rev. Lett. **100**, 167207 (2008).

[21] H. J. Xiang and M.-H. Whangbo, Phys. Rev. B **75**, 052407 (2007).

[22] In our standard Metropolis MC simulations, we consider a conventional cubic cell with 16 spin sites. For one MC simulation, we first generate a random spin configuration. Then we decrease

the system temperature from 100 K to 0.1 K gradually. We repeat several MC simulations to confirm the spin ground state obtained from our MC simulations. If we do not include the single-ion anisotropy and the effect of the DM interaction, the ground state is a perfect isotropic ferromagnetic state. If we include only the DM interaction, the ground state is the same because of the collinearity of the state.
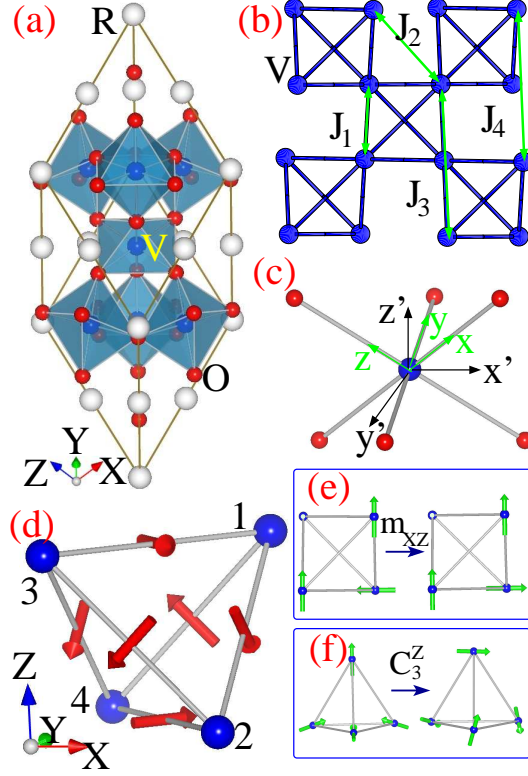
FIG. 1: (a) The crystal structure of $R_2V_2O_7$. The global coordinate system XYZ is indicated. (b) The spin exchange paths between V^{4+} ions. (c) The two local coordinate systems used for the ideal VO_6 octahedron. The xyz coordinate system is defined for the ideal VO_6 octahedron with the x, y and z axes taken along the V-O bonds. In the $x'y'z'$ coordinate system, the z' axis is taken along one three-fold rotational axis of the ideal VO_6 octahedron. In $R_2V_2O_7$ each VO_6 octahedron is axially compressed slightly with only one three-fold rotational axis. (d) The DM vectors $\mathbf{D}_{ij}$ with $i < j$ of the V tetrahedron, where i and j denote the V site labels. (e) The two spin configurations used to extract the DM parameter. (f) The two spin configurations used to extract the single-ion anisotropy parameter.
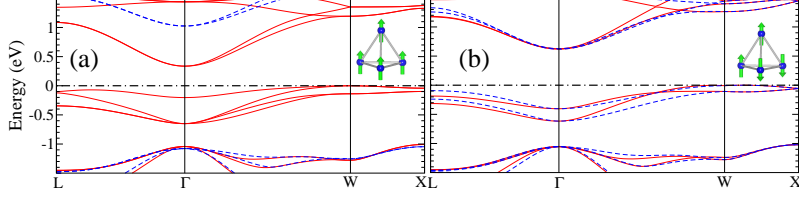
FIG. 2: (color online) (a) The band structure of the FM state from the DFT+U calculation. (b) The band structure of the AFM state (with two up- and two down-spins in each V_4 tetrahedron) from the DFT+U calculation. Solid lines and dashed lines represent up-spin and down-spin bands, respectively.
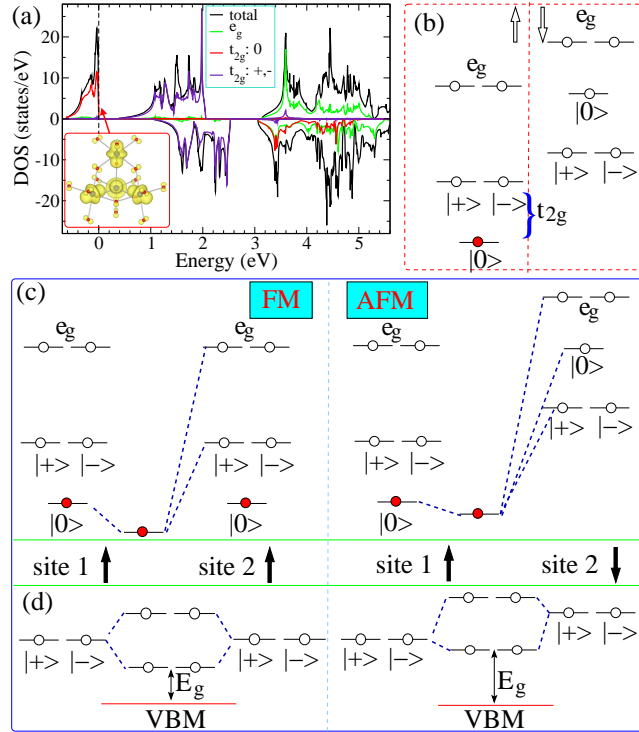

FIG. 3: (color online) (a) The total and partial density of states of the FM state from the DFT+U calculation. The inset shows the density distribution associated with the occupied V $3d^1$ states. (b) A schematic illustration of electron configuration of the V^{4+} ion. (c) The interactions between the 3d-states of two adjacent V^{4+} ions when their spins have the FM and AFM arrangements. Only the hopping processes which lead to the overall energy lowering of the up-spin a_{1g} state of the spin site 1 are shown. (d) The interactions between the 3d-states of two adjacent V^{4+} ions leading to the CBM positions when their spins have the FM and AFM arrangements.
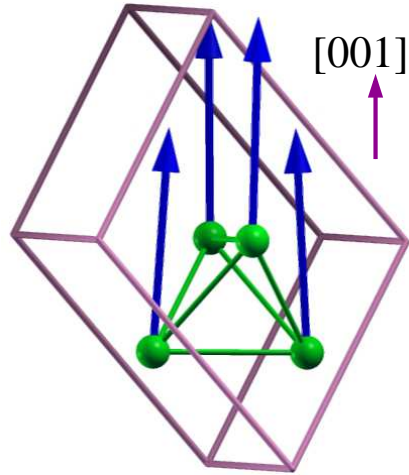
12

FIG. 4: (color online) The spin configuration of the magnetic ground state of $R_2V_2O_7$ from the Monte Carlo simulated annealing method.